EPR and ENDOR Studies of X-Irradiated Single Crystals of Deoxycytidine 5′-Phosphate Monohydrate at 10 and 77 K

David M. Close*

Physics Department, East Tennessee State University, P.O. Box 70652, Johnson City, Tennessee 37614

Eli O. Hole and Einar Sagstuen

Department of Physics, University of Oslo, P.O. Box 1048, Blindern N-0316 Oslo, Norway

William H. Nelson

Department of Physics and Astronomy, Georgia State University, Atlanta, Georgia 30303

Received: March 24, 1998; In Final Form: June 3, 1998

The EPR spectra of single crystals of deoxycytidine 5′-phosphate monohydrate (5′dCMP), X-irradiated at 10 K, exhibit signals from several distinct radical species. Analysis of the ENDOR spectra from two of these radicals indicates that these result from oxidation and reduction of the cytosine base. The reduced species exhibits hyperfine coupling to the C6−H_α proton, and an additional small exchangeable hyperfine coupling from the N3−H proton. No additional couplings that may be associated with protonation of the amino group have been observed. Since the native molecule is protonated at N3, it appears that reduction of the cytosine base does not result in any further protonation. The oxidized species exhibits hyperfine couplings to C5−H_α and C1′−H_β, and two small exchangeable couplings from the C4−NH_2 protons. Since no hyperfine coupling to N3−H was observed, the oxidized species is believed to be the N3−H deprotonated cation. At high X-ray dose there is also evidence for both C5 and C6 H-addition radicals at 10 K. The fate of these radicals has been studied under controlled warming conditions. Attempts have been made to relate the fate of the low-temperature radicals with several radicals that have been detected previously at 77 K and at room temperature.

Introduction

One consequence of the direct effects of ionizing radiation on DNA is the production of electron loss and electron gain centers. An important problem in the field of radiation biology is the determination of the chemical nature and distribution of these initial damage sites in DNA. Electron paramagnetic resonance (EPR) spectroscopy have been used extensively in this effort since this technique is able to characterize the free radicals formed when DNA is exposed to ionizing radiation.

One aspect of these studies has been to characterize the initial electron loss (reduction) products in DNA. At one time it was thought that thymine was the primary reduction site in DNA.[1] However, results by Hüttermann and co-workers,[2] by Bernhard and co-workers,[3] and by Sevilla and co-workers[4] now suggest that cytosine may be the primary reduction site in DNA. Furthermore, dissimilarities in the EPR spectrum from monomers and oligomers of cytosine have focused attention on the protonation state of the cytosine anion.[5]

Numerous EPR studies have been performed on cytosine derivatives. Reviews by Close,[6] Bernhard,[7] and Becker and Sevilla[8] cover most of the results on radical ions and their reactions in cytosine derivatives. While many species formed by oxidation and reduction of cytosine have been reported, the actual protonation states of these products are largely unknown. Steenken has proposed that proton-transfer reactions may be important for the stabilization of the initial DNA ion radicals.[9] To study these proton-transfer reaction schemes, one needs to determine the protonation states of the reduction and oxidation products of cytosine in various chemical environments.

Electron nuclear double resonance (ENDOR) spectroscopy has been very useful in our group's effort to determine the protonation states of various DNA base constituents. A recently completed study on single crystals of cytosine monohydrate revealed the cytosine anion to be protonated at N3 (the small >N3−H and −N4−H_2 proton couplings were detected and characterized), while the cytosine cation to be deprotonated at N1 (the amino protons were characterized by ENDOR).[10] The present work concerns EPR/ENDOR reinvestigations of single crystals of deoxycytidine 5′-phosphate monohydrate (5′dCMP). In a previous study of 5′dCMP, hereafter referred to as (I), the cytosine base reduction and oxidation products were discussed,[11] though the protonation states of these products were not determined. In the present work, the actual protonation states of the primary one-electron oxidation and reduction products in 5′dCMP have been established. Furthermore, aided by additional experimental results, an overview of the radical products trapped, and the transformation these radicals undergo, is presented.

Some recent EPR work on 5′dCMP in frozen solution at 77 K has relevance to the present study. In D_2O the spectrum consists of three components, (1) matrix OD radicals, (2) the base anion, and (3) the C1′ H-abstraction radical.[12] Laser photoionization of cytosine and its derivatives has been used to generate parent radical cations.[13] In cytosine either the π-cation or its N1-deprotonated form is observed. However in N1-substituted derivatives such as 5′dCMP, the parent cations give rise to C1′ H-abstraction radicals even at 77 K.

* To whom correspondence should be addressed: phone, 423-439-5646; FAX, 423-439-6905; E-mail, CLOSED@ETSU.EDU.

S1089-5639(98)01610-7 CCC: $15.00
Published on Web 07/31/1998

Materials and Methods

5′dCMP (structure I) was purchased from Sigma Chemical Company and used without further purification. Single crystals were grown by slow evaporation from either H_2O or D_2O. The crystals are orthorhombic, belonging to space group $P2_12_12_1$.[14] Most of the data were taken by rotating the crystals about the three crystallographic axes. In some cases, however, a skewed axis was used to aid in resolving the Schonland ambiguity in the hyperfine coupling tensors.[15]

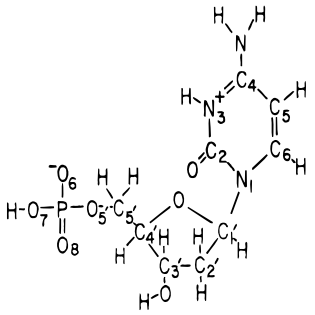

Structure I

The X-band EPR/ENDOR experiments were performed at the University of Rochester. The use of a Cryo-Tip cavity, which allows for irradiations of crystals at temperatures of 10 K or higher, and EPR or ENDOR data acquisition at ∼6 K or higher, has been described elsewhere.[16] Controlled warming EPR eperiments were conducted by warming the irradiated crystals from 10 to 300 K. EPR experiments were also performed by irradiating the crystals at 77 K. Methods of crystal orientation, data collection, and analysis have been previously described.[17]

K-band EPR, ENDOR, and field-swept ENDOR (FSE) experiments were performed at Georgia State University on equipment previously described.[18] The crystals were X-irradiated to doses in the range of 15−100 kGy at 10 K and maintained at this temperature for data collection. Computer simulations of composite EPR spectra as well as of powder spectra were made using Maruani's program with parameters described in the text.[19]

A large number of hyperfine coupling tensors are reported in this work. The extensive data for each coupling and plots comparing the angular variations of the ENDOR data with those calculated from the coupling tensors have not been included. These plots are available upon request from the authors.

Results and Analysis

Reduction of the Cytosine Base (Radical R1). Typical ENDOR and field-swept ENDOR (FSE) spectra of single crystals of 5′dCMP, X-irradiated and observed at 10 K, are shown in Figure 1. Three ENDOR lines were associated with radical **R1** in normal crystals as established from FSE spectra as well as from thermal annealing experiments. These ENDOR lines decay on warming to ca. 100 K. Hyperfine couplings obtained from the ENDOR data are given in Table 1.

Tensor **1a** is characteristic of an interaction between an unpaired π-electron spin density and a $>\dot{C}6-H_\alpha$ fragment. The eigenvectors for the intermediate and minimum principal values are close to the directions for the cytosine ring plane normal and the >C6−H bond direction. Using a Q-value of −72.8 MHz[7] in the McConnell relation,[20] the spin density at C6 was computed to be 0.56. Bernhard has argued that the dipolar coupling tensor is more reliable than the isotropic coupling in estimating π-spin densities at α-carbons.[21] From the dipolar coupling tensor in Table 1, Bernhard's relation yields a spin density of 0.51.

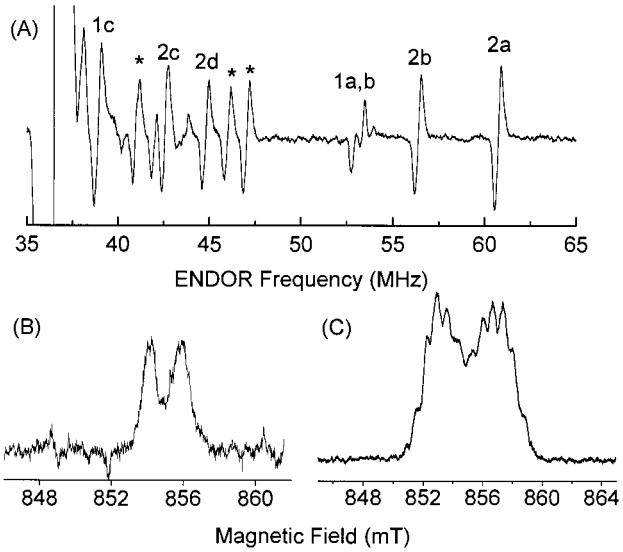

Figure 1. (A) K-band ENDOR spectrum from a nondeuterated single crystal of 5′dCMP, X-irradiated and measured at 10 K. Low-dose (crystal irradiated with 55 kVp (kilovolts peak), 10 mA X-rays for 1 h) study for rotation about the ⟨a⟩ crystallographic axis, H_o parallel to the ⟨c⟩ axis. ENDOR lines marked ∗ are from the alkoxy radical (ref 24). (B) The ENDOR lines at ca. 53.5 MHz in Figure 1A, showing the characteristic additional splitting associated with radical **R1a**. The FSE spectrum from this line is poorly resolved at this crystallographic orientation. FSE spectrum from the same ENDOR line for H_o parallel to the ⟨b⟩ crystallographic axis, showing the narrow EPR doublet from radical **R1a** (ENDOR frequency now 55.66 MHz). (C) FSE spectrum from the ENDOR line at 60.91 MHz. ENDOR lines at 42.75, 44.99, and 56.55 MHz gave a similar broad FSE pattern characteristic of radical **R2b**.

In the previous X-band study (I), when the $>\dot{C}6-H_\alpha$ coupling was analyzed, it was noted that in some crystallographic orientations, a second set of ENDOR lines was observed (particularly with H_o in the ⟨ac⟩-crystallographic plane). This led to some small inaccuracies in determining the coupling tensor. In the present study care was taken to follow the second set of hyperfine couplings in all three crystallographic planes. The results for this second coupling are given in Table 1 as **1b.**

For tensor **1c**, which was not observed in (I), the eigenvectors for the intermediate and minimum principal values are close to the directions for the cytosine ring plane normal and the >N3−H bond direction. In partially deuterated crystals this hyperfine coupling was not present, indicating a coupling to a nitrogen-bonded proton. Therefore tensor **1c** is associated with the N3−H proton coupling. With a Q-value of −80 MHz[22] in the McConnell relation,[20] the π-spin density at N3 is calculated to be 0.07. These results then are almost identical to the N3−H_α coupling associated with the cytosine anion observed in cytosine monohydrate.[10]

In the previous study (I) the reduction product was considered to have one of the following possible structures (structures **R1a** and **R1b**). In the cytosine monohydrate study, additional weak couplings were associated with the $N4H_2$ protons.[10] These couplings were even weaker than the N3−H coupling. In the present study there is too much interference from other weak hyperfine couplings to positively identify any additional hyperfine couplings associated with radical **R1**.

Consequently, it seems that the best choice for radical **R1** is structure **R1a** on the basis of the fact that the N3−H coupling

TABLE 1: Hyperfine Couplings for Radical R1 Formed in 5′dCMP Single Crystals, X-Irradiated and Observed at 10 K

			eigenvectors[b]			
tensor	isotropic value[a]	principal values	⟨*a*⟩	⟨*b*⟩	⟨*c*⟩	($\Delta\psi$),[c] deg
		−64.9(3)	0.702(3)	−0.599(5)	0.119(1)	
1a	−40.8(3)	−36.3(1)	0.202(7)	0.440(6)	0.875(3)	
			(0.136)	(0.492)	(0.860)[d]	4.8
		−21.3(3)	0.577(3)	0.669(6)	−0.469(5)	
			(0.619)	(0.635)	(−0.462)[e]	3.1
		−63.2(6)	0.815(10)	−0.542(17)	0.205(4)	
1b	−39.2(5)	−36.7(2)	0.171(18)	0.564(10)	0.808(6)	5.4
		−17.6(6)	−0.554(11)	−0.622(15)	0.552(8)	6.5
		−10.4(2)	0.498(20)	−0.865(13)	0.062(49)	
1c	−5.8(2)	−5.4(3)	0.320(51)	0.250(58)	0.914(27)	
		−1.6(3)	0.806(24)	0.436(24)	−0.401(59)	
			(0.740)	(0.519)	(−0.429)[f]	6.3

[a] Hyperfine couplings are in MHz. Uncertainties in the last digit(s) are given in parentheses, quoted at the 95% confidence level. [b] Eigenvectors here are for crystallographic site *(l, m, n)*. The other three symmetry related sites are given by (l, $\bar{m}$, $\bar{n}$), ($\bar{l}$, m, $\bar{n}$), ($\bar{l}$, $\bar{m}$, n). [c] $\Delta\psi$ is the angle between a specific principal value and the expected direction computed from the coordinates of the native molecule (ref 14). [d] The expected direction of the C6 2pπ orbital (the perpendicular to the pyrimidine plane). [e] The expected direction of the C6−H_α bond (the in-plane bisector of the C5−C6−N1 bond). [f] The expected direction of the N3−H bond (taken from the N3···O8(P) direction).

TABLE 2: Hyperfine Couplings for Radical R2 Formed in 5′dCMP Single Crystals, X-Irradiated and Observed at 10 K

			eigenvectors[b]			
tensor	isotropic value[a]	principal values	⟨*a*⟩	⟨*b*⟩	⟨*c*⟩	($\Delta\psi$),[c] deg
		−62.6(1)	0.156(9)	0.833(4)	−0.531(2)	
2a	−41.2(1)	−42.9(1)	0.170(6)	0.507(8)	0.845(3)	
			(0.165)	(0.500)	(0.850)[d]	2.4
		−18.0(1)	0.973(7)	−0.222(13)	−0.062(29)	
			(0.976)	(−0.206)	(−0.068)[e]	2.1
		46.8(3)	0.490(23)	−0.848(12)	−0.201(13)	
2b	41.9(5)	39.5(1)	0.259(104)	0.362(37)	−0.895(31)	
		39.5(1)	0.832(27)	0.387(55)	0.397(61)	
		−18.6(1)	0.245(13)	0.841(17)	−0.483(106)	
2c	−12.4(1)	−16.4(1)	0.025(46)	0.492(64)	0.870(1)	
			(0.130)	(0.527)	(0.840)[f]	6.6
		−2.3(2)	−0.969(3)	0.225(5)	−0.100(57)	
			(−0.986)	(0.088)	(−0.144)[g]	8.3
		−24.5(1)	0.797(3)	−0.524(6)	0.299(6)	
2d	−14.5(1)	−16.8(1)	0.059(8)	0.561(13)	0.826(9)	4.3
		−2.3(2)	−0.601(4)	−0.641(5)	0.478(4)	
			(−0.681)	(−0.552)	(0.481)[h]	6.8

[a] Hyperfine couplings are in MHz. Uncertainties in the last digit(s) are given in parentheses, quoted at the 95% confidence level. [b] Eigenvectors here are for crystallographic site *(l, m, n)*. The other three symmetry related sites are given by (1, $\bar{m}$, $\bar{n}$), ($\bar{1}$, m, $\bar{n}$), ($\bar{1}$, $\bar{m}$, n). [c] $\Delta\psi$ is the angle between a specific principal value and the expected direction computed from the coordinates of the native molecule (ref 14). [d] The expected direction of the C5 2pπ orbital (the perpendicular to the pyrimidine plane). [e] The expected direction of the C5−H_α bond (the in-plane bisector of the C5−C6−N1 bond). [f] The expected direction of the N4 2pπ orbital (the perpendicular to the pyrimidine plane). [g] The expected direction of the N4−H1 bond. [h] The expected direction of the N4−H2 bond.

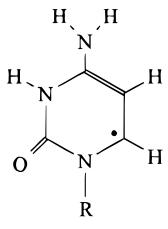

R1a

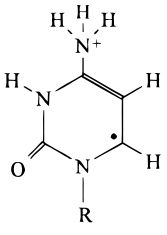

R1b

has been observed and that no additional coupling that might be associated with protonation of the amino group has been observed.

Oxidation of the Cytosine Base (Radical R2). Four ENDOR lines were associated with radical **R2** in normal crystals (grown from H_2O) as established from field-swept ENDOR spectra (Figure 1) as well as from thermal annealing experiments. These ENDOR lines decay on warming to ca. 60 K. Hyperfine couplings obtained from the ENDOR data are given in Table 2.

The eigenvectors for the intermediate and minimum principal values of the coupling with the largest anisotropy (**2a** in Table 2) are close to the directions for the cytosine ring plane normal and the >C5−H bond direction. This coupling then is associated with the >C5−H_α proton. Using a Q-value of −72.8 MHz[7] in the McConnell relation,[20] the spin density at C5 was computed to be 0.56, whereas if the dipolar coupling tensor is used[21] the spin density at C5 is computed to be 0.60.

The second hyperfine coupling (**2b** in Table 2) is characteristic of a β-proton with a sizable isotropic interaction (ca. 1.4 mT). Normally one assumes that a cytosine ring proton cannot be sufficiently far out of the ring plane to be responsible for such a large hyperfine coupling. Therefore this coupling was assumed in (I) to be due to the C1′−H_β proton. This is reasonable only if radical **R2** has significant spin density at N1, which is discussed below.

Two additional weak ENDOR lines can be linked to the base oxidation product using FSE techniques (Table 2). Both couplings are exchangeable, typical of couplings of N−H_α

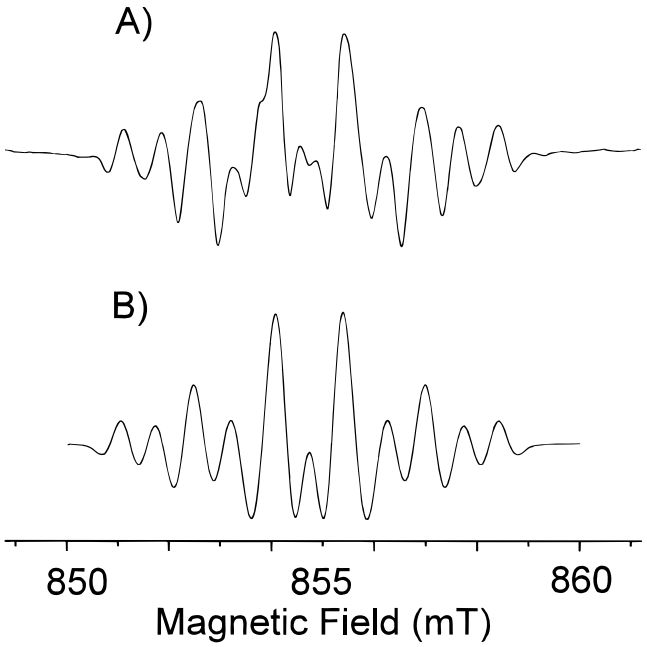

Figure 2. (A) K-band EPR spectrum from a deuterated single crystal, X-irradiated (55 kVp, 10 mA for 4.5 h) and measured at 10 K. H_o parallel to the $\langle c \rangle$ crystallographic axis. The spectrum is composed mainly of a 1.25 mT doublet from radical **R1a** and a broad EPR signal from radical **R2b.** (B) Simulation of the EPR spectrum using the program by Maruani (ref 19). For Radical **R1a** the C6−H_α tensor in Table 1 was used, together with a cytosine anion **g**-tensor suggested in ref 10. For radical **R2b** tensors **2a** and **2b** from Table 2 were used along with two axially symmetric nitrogen hyperfine couplings with principal values of (1.7, 0.1, 0.1) and (0.8, 0.1, 0.1) mT.

fragments, and exhibit eigenvectors for the intermediate principal value close to the direction of the ring perpendicular. The eigenvectors for the minimum principal values of these hyperfine couplings are close to the two N4−H proton directions. The isotropic values of the two tensors are very similar indicating N4 spin density of 0.17 ± 0.01 (with a Q-value of −80 MHz).

Attempts have been made to determine nitrogen spin densities exhibited by radical **R2** from the EPR spectra (Figure 2). The spectra chosen for simulations were for $H_o \parallel$ to $\langle c \rangle$ plane, D_2O crystals, irradiated at low X-ray dose. One can see from the angular variations of the EPR spectra that there are contributions from hyperfine couplings not seen by ENDOR. In particular a maximum spectral width is seen in a direction perpendicular to the pyrimidine plane. This feature is characteristic of 2pπ nitrogen hyperfine coupling. The best EPR simulations were obtained with the ENDOR tensors in Table 2 and two additional nitrogen hyperfine couplings with $A_{iso}(N1) = 0.63$ mT and a second smaller $A_{iso}(N4) = 0.33$ mT.

Using this value of $A_{iso}(N4) = 0.33$ mT and the $\rho(N4) = 0.17 \pm 0.01$, one has a $Q^N = 1.9 \pm 0.1$ mT. With this Q-value, the N1 spin density is estimated to be 0.30, which is the same as previously calculated for the cytosine cation.[10] Finally, the β-proton coupling (**2b** in Table 2) can be used to estimate the torsion angle from the approximate formula

$$A_{iso}(H_\beta) = \rho(N1)\, B_2 \cos^2 \theta \qquad (1)$$

with $B_2 \sim 170$ MHz,[23] which gives $\theta = 26 \pm 4°$. From the crystal structure one can determine that the torsion angle between C6−N1−C1′−H_β is 101.4°, while the torsion angle between C2−N1−C1′−H_β is −70.3°. This indicates some nonplanarity in the N1 bonding. If one assumes that the nitrogen 2pπ orbital is perpendicular to the C2−N1−C6 plane, then the torsion angle between this perpendicular and the C1′−H direction is calculated to be 15.8°. Considering the approximate nature of eq 1 and the constants used, this agreement is quite satisfactory.

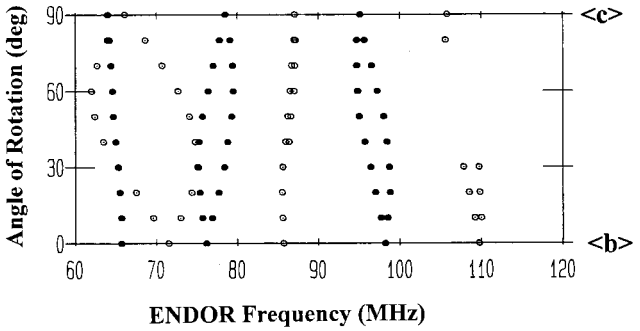

Figure 3. Angular variations of the K-band ENDOR spectra from a single crystal of 5′dCMP, X-irradiated and measured at 10 K. High-dose experiment (crystal X-irradiated 4.25 h with 55 kVp X-rays at 10 mA) for rotation about the $\langle a \rangle$ crystallographic axis. Only the high-field ENDOR lines from radicals **R4** and **R5** are shown here.

To assign a structure to radical **R2** one must account for appreciable spin density on N1 and C5 and modest spin density on N4. No coupling was observed that can be associated with the N3−H proton for this radical. The small N3 coupling is in accord with recent results by Malone et al.[13] They report no spectral changes on N3 methyl substitution in various cytosine π-cations. Therefore it seems most likely that the oxidation product observed at 10 K in 5′dCMP is radical **R2b**, the N3-deprotonated cation.

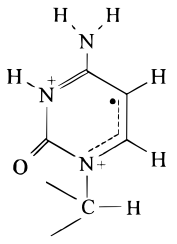

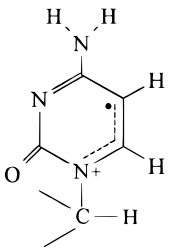

Oxidation of the Deoxyribose Moiety (Radical R3). The only identified product associated with radiation damage to the deoxyribose moiety is a secondary alkoxy radical observed at 10 K and stable on warming to ca. 65 K. This radical was correctly identified by Box et al.,[24] and although ENDOR lines from this radical were detected in the present work (Figure 1), no new experimental results on this radical are reported here. It is important to note, however, that this radical exhibits a number of weak hyperfine couplings that appear only 5−8 MHz from the free proton ENDOR signal (36.5 MHz at K-band), which interfered with the weak couplings from radicals **R1** and **R2**.

H-Addition Radicals (R4 and R5). In crystals given a high X-ray dose at 10 K, one sees, in addition to the three primary radicals discussed above, several ENDOR lines above 65 MHz. In Figure 3 one sees the angular variations of these ENDOR lines for the rot $\langle a \rangle$ plane. Although ENDOR lines were observed at several orientations in other planes, the resonances were too weak to allow for the calculation of hyperfine coupling tensors. However, enough information is available from this single plane of data to make reasonable radical assignments.

FSE results for the orientation $H_o \parallel \langle b \rangle$ show that the ENDOR lines at 72.6, 85.7, and 109.6 MHz belong to the same radical species (radical **R4)**. The two high-frequency lines represent

β-proton interactions of 3.5 and >5.1 mT. At some of the angles recorded above 100 MHz, the ENDOR lines were too weak to be observed. There are, however, data at enough orientations to be confident about the presence of this β-proton interaction. Such large couplings are typically seen in cytosine C5═C6 H-addition products.[7] For example, the C6−H_{add} radical in 1MeC has two isotropic β-proton couplings of 4.78 and 5.13 mT.[25]

The hyperfine coupling at 72.6 MHz (for $H_o \parallel \langle b \rangle$ in Figure 3) has an angular variation characteristic of an α-proton interaction. Actually one sees that the plot has the same anisotropy as the >C5−H_α proton interaction of radical **2a.** This then is sufficient to establish that radical **R4** is the C6−H_{add} radical.

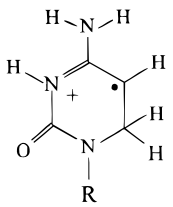

R4

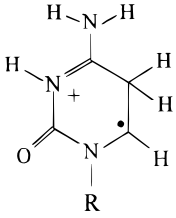

R5

The other three high-frequency ENDOR lines in Figure 3 are also linked by FSE to a single radical species (**R5**). The lines at 76.2 and 98.2 MHz correspond to β-proton interactions of 2.72 and 3.51 mT. The single line at ca. 66 MHz is the C6−H_α coupling. This coupling has the same angular variation as the C6−H_α coupling of radical **R1** for this plane of data. The hyperfine couplings observed for this radical are typical of those observed for cytosine C5−H_{add} radicals.[7] Therefore, it seems safe to conclude that radical **R5** is indeed the C5−H_{add} radical shown above.

It is important to point out here that the evidence for H-addition radicals at 10 K comes mainly from the ENDOR results. There is only weak evidence for either H-addition radical in any of the EPR spectra at 10 K. There is EPR evidence for a C6−H_{add} radical at temperatures above 100 K but with slightly different β-proton hyperfine couplings. At room temperature only the C6−H_{add} radical is observed. The two β-proton hyperfine couplings are close to being equivalent (4.09 mT).[26]

Unidentified Radicals Species. In addition to the 12 hyperfine couplings discussed above, and 4 or 5 small couplings associated with the secondary alkoxy radical, there are several additional hyperfine couplings to which no radicals species has been assigned. From one small ENDOR coupling a hyperfine coupling tensor with principal values of 21.3, 11.6, and 10.3 MHz has been obtained. The FSE spectrum from this coupling was poorly resolved. This coupling most likely is a small β-proton interaction from some unidentified sugar radical.

There is one more large hyperfine coupling that was obtained from the high-dose plane of data. For rotation about the $\langle a \rangle$ axis, this coupling varies from 1.68 to 3.15 mT. The FSE is well-resolved and shown a single doublet. Unfortunately this coupling was too weak to be observed in the other data sets, and so no additional information is available. This large anisotropic coupling is most likely from a sugar H-abstraction radical. A recent paper on sugar radicals summarizes the spectral features of the five H-abstraction radicals.[27] C5′ H-abstraction radicals generally have a large C5′−H_α anisotropic hyperfine coupling and only very small β-proton interactions. While this fits the data currently available, it is premature to speculate on a radical assignment without the complete hyperfine coupling tensor.

Radicals Observed at 10 K, Summary. The primary radiation induced products in 5′dCMP are therefore (1) reduction of the base (**R1a**), (2) oxidation of the base resulting in the N3-deprotonated cation (**R2b**), (3) oxidation of the deoxyribose moiety, resulting in a secondary alkoxy radical at O3′, (4) C5═C6 H-addition radicals **R4** and **R5** (at least at high radiation dose), and (5) perhaps one or two unidentified sugar radicals.

Radicals at 77 K (R6). An interesting radical observed in 5′dCMP by irradiation at 77 K by Krilov and Herak[28] has the structure $\dot{C}5'(H_2)-C4'(H)<$. The analysis performed by Krilov and Herak on the EPR data produced one isotropic hyperfine coupling of 3.6 mT and two anisotropic couplings with principal values of −2.97, −2.04, and −1.40 mT. These principal values deviate from normal α-proton anisotropic couplings since only the mean value of the two anisotropic couplings was measured. The proper hyperfine couplings for the methylene protons, suitable for EPR spectral simulation, were obtained by the following procedure.

Our analysis of the X-band EPR spectra at 77 K produced a hyperfine coupling tensor with principal values of −2.94, −1.97, and −1.44 mT, in good agreement with the results of Krilov and Herak.[28] The direction cosine associated with A_{max} is essentially parallel to the C4′−C5′ direction. A principal axis system was chosen that represents the direction of the π-electron orbital, the C4′−C5′ bond direction, and a third direction perpendicular to the first two axes. Then the direction of A_{mid} was chosen as the direction of the π-orbital. Assuming ideal sp^2 structure, the other principal values of 1.44 and 2.94 mT can be transformed to the in-plane principal values of the individual methylene protons using

$$(A_{min})^2 \cos^2 30° + (A_{max})^2 \cos^2 60° = (1.44)^2 \qquad (2)$$

$$(A_{min})^2 \cos^2 60° + (A_{max})^2 \cos^2 30° = (2.94)^2 \qquad (3)$$

The solutions are $A_{min} = 1.06$ mT and $A_{max} = 3.45$ mT. This agrees well with the experimental >C−H_α values of 1.07, 2.20, 3.30 mT.[29]

Using the individual hyperfine couplings for each methylene proton, and a 3.6 mT β-proton coupling, one can simulate the EPR spectrum for radical **R6**. Figure 4 shows the EPR spectrum for H_o along the $\langle b \rangle$ crystallographic axis. Comparing this spectrum with the spectrum shown by Krilov and Herak, one notes the increased resolution of the former at low EPR field modulation. Also shown is the simulation of the EPR powder spectrum for this radical, which should be compared the EPR spectra from a number of cytosine derivatives shown in a recent paper by Malone et al.[13]

Discussion

Reduction of Cytosine. A number of cytosine reduction products have been characterized by detailed ENDOR experiments on single crystals X-irradiated and observed at or near liquid helium temperatures. The results are summarized in Table 3.

In cytosine monohydrate the native molecule is neutral (not protonated at N3) The first entry in Table 3 is the reduction product observed in this crystal.[10] The reduction product is protonated at N3. The second entry represents a reduction product in the same crystal formed by net H-addition to the exocyclic O2 site.[30] The distinguishing feature of this product is the rather low spin density on C6.

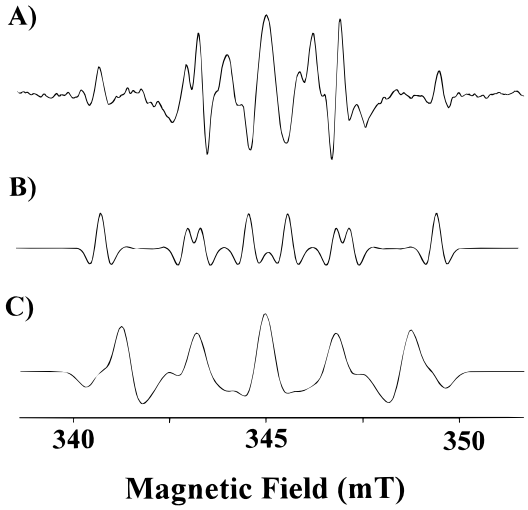

Figure 4. (A) X-band EPR spectra from a single crystal of 5′dCMP, X-irradiated and measured at 77 K, for H_o parallel to the ⟨*b*⟩ crystallographic axis. This spectrum should be compared with the overmodulated EPR spectrum in ref 28 (Figure 1). (B) Simulation of the EPR spectrum of radical **R6** for H_o parallel to the ⟨*b*⟩ crystallographic axis, using the hyperfine couplings described in the text. (C) Simulation of the EPR powder spectrum of radical **R6**.

TABLE 3: Cytosine Reduction Products

system	radical[a]	A_{iso}[b]	principal values[c]	ρ[d]	ref
C·H_2O	C_a+3	−37.8	−24.7, 2.3, 22.5	C6(0.52)	10
C·H_2O	C_a+2	−26.7	−15.3, 2.0, 13.3	C6(0.36)	30
3′CMP	C_a^+	−36.0	−23.2, 2.0, 21.3	C6(0.49)	31
C·HCl	C_a^++4	−34.4	−19.0, 1.1, 18.0	C6(0.47)	33
C·HCl	C_a^+	−39.0	−22.8, 2.6, 20.2	C6(0.52)	33
1MeC·5FU	C_a+3	−38.6	−23.9, 4.0, 19.9	C6(0.51)	51
5′dCMP	C_a^+	−40.8	−24.1, 4.5, 19.5	C6(0.51)	this work

[a] Radical assignment here using the notation given by Bernhard in ref 7. [b] Isotropic hyperfine coupling in MHz. [c] Dipolar components of the hyperfine coupling tensor (in MHz). [d] Major site of unpaired spin density, calculated from the dipolar hyperfine coupling tensor.

The next four entries in Table 4 are for crystals in which the native molecule is protonated at N3. In Box's paper on the ENDOR analysis of 3′CMP the reduction product is shown as a negative ion (i.e., deprotonated at N3 after electron addition).[31] Close[32] and Bernhard[7] have both pointed out that this species actually remains protonated at N3.

The recent study of cytosine hydrochloride provides two interesting reduction products.[33] At low doses and low temperatures, one observes the neutral reduction product (molecule remains protonated at N3 after electron addition). At high doses one also observes a reduction product that is further protonated at the exocyclic NH_2 group. This species has been previously inferred from frozen solution studies.[5] One further point to note is the remarkable similarity between the N3-protonated species observed in cytosine derivatives. Adding the present work on 5′dCMP, there are six reduction species in cytosine with nearly identical spin density on C6.

Another point to consider here is the multiple set of closely spaced ENDOR lines observed for some reduction products. These were first noted in (I). Similar results have also been observed for reduction products in single crystals of guanine·HCl·H_2O[34] and guanine·HCl·$2H_2O$.[18] It is quite likely that these closely related reduction species represent slight differences in radical conformation. McCalley and Kwiram[35] report a similar effect in an ENDOR study of malonic acid at 4.2 K. They observe one set of closely matched pairs of ENDOR lines from the RCHR radical. This doubling is a consequence of the absence of the crystallographic inversion center present at room temperature. It is not known if there is a similar loss of crystallographic symmetry upon cooling in the crystals we have studied.

TABLE 4: Cytosine Oxidation Products

system	radical[a]	A_{iso}[b]	principal values[c]	ρ[d]	ref
C·H_2O	C_c−1	−41.3	−22.8, −0.8, 22.2	C5(0.56)	10
C·HCl	C_c^+−4	−27.3	−11.6, −2.0, 13.7	C5(0.36)	33
C·HCl	C_c^+−3	−41.4	−22.9, −0.9, 21.7	C5(0.56)	33
C·HCl	C_c^+−1	−41.5	−25.2, −0.3, 24.9	C5(0.64)	33
5′dCMP	C_c^+−3	−41.2	−21.4, −1.7, 23.2	C5(0.60)	this work

[a] Radical assignment here using the notation given by Bernhard (ref 7). [b] Isotropic hyperfine coupling in MHz. [c] Dipolar components of the hyperfine coupling tensor in MHz. [d] Main site of unpaired spin density, calculated from the dipolar hyperfine coupling tensor.

Oxidation of Cytosine. The characteristics of cytosine oxidation products are listed in Table 4. The first entry represents oxidation of the neutral cytosine base. This radical is stabilized by deprotonation at N1.[10] The next three entries are for oxidation products observed in cytosine hydrochloride in which the base is protonated at N3 in the native molecule. Cations are observed that are stabilized by deprotonation at N4, N3, and N1.[33] The final entry is for 5′dCMP where it is believed that the oxidation product formed is the N3-deprotonated cation. One notes that except for the N4-deprotonated cation in C·HCl, the other entries have very similar spin densities at C5. One feature to note in Table 4 is that all the electron loss centers here are deprotonated. In our previous work we have noted that cations of guanine and adenine tend to deprotonate at the exocyclic amino group.[6] In C·HCl the dominant oxidation product is indeed the amino-deprotonated cation, but two other sites of deprotonation are also observed. This likely reflects the fact that none of the available sites in C·HCl are hydrogen bonded to good proton acceptors.

It has been shown that proton-transfer networks that promote the separation of charge and spin are important in stabilizing radicals.[36] This provides the means of returning ionization sites to their original charge state and effectively inhibiting recombination. One would like to see if the hydrogen-bonding network in 5′dCMP might be used to explain why the radical cation is stabilized by deprotonation at N3 rather than, say, at C1′ as is observed in solution.

In 5′dCMP the crystal structure shows that there is an intricate hydrogen-bonding network involving N3 and the phosphate group, (N3−H···O8−P−O7−H···O3′−H···Ow−H···O2).[14] This network provides a convenient path to shuttle the excess positive charge (via N3−H deprotonation) far away from the original site of oxidation. Indeed, if the charge moves through the four hydrogen bonds here it will end up 9.3 Å from the original oxidation site. On the other hand, C1′−H is not involved in H-bonding with neighbors. The crystal structure does not show any good proton acceptors within 3 Å of C1′−H.

H-Addition Radicals. In previous EPR studies it has commonly been assumed that the electron adduct is the precursor to the base H-addition radicals. One often sees the cytosine electron adduct signal decay on warming to 100−150 K at which time the H-adduct signals appear to grow in. However, detailed ENDOR studies have shown that when base electron adducts are formed they rapidly protonate.[6] At low temperatures one often sees ENDOR signals from the H-adducts. Upon warming, the electron adduct signal often decays with no apparent successor. Therefore in the crystalline state, at least, there does not seem to be a necessary link between the electron adducts and the H-addition radicals.

Sugar Radicals. Identification of an alkoxy radical in 5′dCMP initially led to several incorrect assignments.[37,11]

TABLE 5: Hyperfine Coupling Tensors for the 3αH Radicals in Cytosine Derivatives

hyperfine tensor (MHz)	eigenvectors[b] ⟨a⟩	⟨b⟩	⟨c⟩	(Δψ),[a] deg
	5′dCMP[b]			
	Coupling 1			
−18.78	−0.4264	−0.7908	−0.4392	
−42.96	0.3537	−0.5926	0.7392	10.5[c]
−71.16	−0.8325	0.1532	0.5324	
	Coupling 2			
−19.15	−0.5148	0.5147	0.6356	
−44.24	0.3331	−0.6186	0.7132	13.9[c]
−67.18	0.7900	0.5955	0.1460	
	Coupling 3			
−11.69	−0.4751	0.6613	0.5805	10.8[d]
−25.77	0.2136	−0.5333	0.8051	9.4[c]
−34.93	0.8536	0.5065	0.1216	
	3′CMP[e]			
	Coupling 1			
−13.2	−0.7036	0.3811	0.5997	
−39.6	0.7016	0.5064	0.5013	27.0[f]
−58.9	−0.1127	0.7735	−0.6237	
	Coupling 2			
−18.2	0.4382	−0.8556	0.2755	
−39.7	0.6894	0.5166	0.5078	27.9[f]
−61.3	−0.5768	−0.0326	0.8167	
	Coupling 3			
− 6.9	−0.7026	0.5483	0.4536	39.8[g]
−29.1	0.7071	0.4661	0.5318	20.5[f]
−39.6	−0.0801	−0.6944	0.7152	
	Cytidine[h]			
	Coupling 1			
−20.74	0.014	0.829	0.560	
−43.54	−0.640	−0.423	0.642	16.7[i]
−66.30	−0.768	0.367	−0.525	
	Coupling 2			
−20.34	−0.638	−0.051	−0.768	
−43.38	−0.685	−0.418	0.597	19.3[i]
−68.86	0.352	−0.907	−0.232	
	Coupling 3			
−13.56	−0.087	−0.752	−0.654	1.0[j]
−27.00	−0.510	−0.530	0.677	7.0[i]
−37.16	0.856	−0.392	0.337	
	1-MeT[k]			
	Coupling 1			
−21.0	0.393	0.877	−0.277	
−43.6	0.496	0.052	0.867	
−67.7	0.774	−0.478	−0.415	
	Coupling 2			
−23.1	0.853	0.039	−0.520	
−44.1	0.518	0.053	0.854	
−72.5	0.062	−0.998	0.025	
	Coupling 3			
−13.1	0.490	0.790	−0.369	
−27.1	0.512	0.082	0.855	
−37.4	0.706	−0.608	−0.364	

[a] $\Delta\psi$ is the angle between a specific principal value and the expected direction computed from the coordinates of the native molecule. [b] See ref 44. [c] Direction of ring perpendicular: 0.1654 −0.5004 0.8499. [d] Direction of C6−H_α: −0.6190 0.6353 0.4617. [e] See ref 43. [f] Direction of ring perpendicular: 0.9409 0.2991 0.1584. [g] Direction of C6−H_α: −0.1053 0.6288 0.7704. [h] See ref 42. [i] Direction of ring perpendicular: −0.4210−0.6130 0.6686. [j] Direction of C6−H_α: −0.0786−0.7590−0.6464. [k] See ref 50.

However, ENDOR results by Box et al.,[24] which accounted for one β-proton and three γ-proton couplings, leave no doubt that the alkoxy radical in 5′dCMP is a secondary alkoxy radical located at O3′.

Some time ago it was suggested by Hüttermann[38] that in DNA there is a shift away from damage to the sugar. In a 3′ nucleotide one often observes a Ȯ−C5′ alkoxy radical.[39] If this position is blocked by the attachment of a phosphate group as in a 5′-nucleotide, the site of oxidation may be the secondary alcohol group (as in 5′dCMP).[11] Extrapolating to the polymers, one sees that all alcohol functions are used as phosphoester bonds. Therefore in DNA the site of direct oxidation is most likely the base.

Another common type of sugar damage results in the production of H-abstraction radicals. In the present work there is only weak evidence for any sugar H-abstraction radicals at 10 K. This is surprising since numerous sugar radicals have previously been detected in nucleosides and nucleotides.[27]

Phosphate Damage. To form radical **R6**, it is necessary to cleave the phosphoester bond. This radical is therefore of interest as a possible intermediate in a strand break. Repeated attempts to study this radical below 77 K have failed. The distinctive EPR spectrum of this radical for H_o along the ⟨*b*⟩ axis is not apparent at 10−20 K. Therefore the precursor to this radical has not been observed. A similar radical has been observed by ENDOR in single crystals of 5′dGMP.[40] In this crystal the radical undergoes a reorientation on warming from 10 to 77 K.

Likely pathways for formation of radical **R6** involve dissociative electron capture of the phosphate group.[41] It is commonly assumed, however, that when bases are present electron capture by the phosphate is unlikely. There is therefore likely a split in the reaction pathway, which depends on the thermal energy available during irradiation. At 10 K base electron adducts are stably trapped. On warming, the base electron loss and electron gain products likely recombine, and therefore very few electrons are available to form radical **R6**. On the other hand, when the sample is irradiated at 77 K, enough energy is apparently available for dissociative electron capture of the phosphate ester to produce radical **R6**.

Room-Temperature Radicals (R7). A radical that was first observed in cytidine at room temperature by Hampton and Alexander[42] has the general features

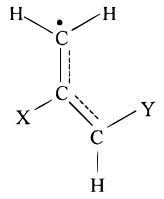

R7a

and is therefore referred to as the 3αH radical. This radical has also been observed in 3′CMP by Bernhard et al.[43] upon annealing to 300 K, and in 5′dCMP by Close et al.[44] by irradiating at room temperature. It has been proposed that this radical is formed in the ribose moiety, although its precise structure, as well as the mechanism of formation, is unknown.[43]

In our study of the 3αH radical in 5′dCMP, we considered the remote possibility that this radical is actually located on the cytosine base.[44] The suggested structure is

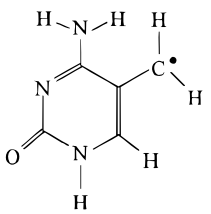

R7b

similar in structure to the thymine allylic radical.[45,46] Table 5

lists the original hyperfine coupling tensors for the 3αH radical along with the direction cosines associated with the C5═C6 region of the cytosine base. One sees that, except for 3′CMP, the fit is very good.

In addition one must ask if there is enough space in this region to replace the C_5 proton with a methyl group. A search was made of the distances between a carbon atom 1.54 Å from C5 and all neighboring molecules in 5′dCMP. There is an oxygen atom (a C2═O) 1.81 Å away and another oxygen (a P−O8) 2.81 Å away. This means that there might be some small distortions necessary to accommodate a methyl group on C5.

Cullis has pointed out that common nucleosides and nucleotides provided by Sigma often contain methylated impurities.[47] The actual 5′dCMP material used for growing crystals has been analyzed, and it does indeed contain approximately 0.04% 5-methyl deoxycytidine as an impurity.[48] If a methylated cytosine impurity is responsible for the 3αH radical, it is necessary to show the following: (1) that the impurity is actually contained in the single crystals, (2) that there is reason to believe that a minor impurity can give rise to a large EPR/ENDOR signal, and (3) that the ENDOR data obtained on the 3αH radical actually fit an allylic cytosine base radical (see Table 3). Experiments to resolve these issues are currently being pursued.

Radical Reactions. The dominant features of the EPR spectrum of 5′dCMP X-irradiated at 10 K are from the base oxidation and reduction products (radicals **R1a** and **R2b**). On warming these species are apparently not involved in any further radical reactions. Their signals disappear without any detectable successors.

A C3′−O alkoxy radical is also present in irradiated 5′dCMP at 10 K along with small quantities of the C5 and C6 H-addition radicals. Oxidation of the sugar produces a cation, which in turn deprotonates to give the alkoxy radical.

$$>C-OH \rightarrow (>C-OH)^+ + e^- \quad (4)$$

$$(>C-OH)^+ \rightarrow >C-\dot{O} + H^+ \quad (5)$$

The H^+ here is H-bonded to a water molecule, which in turn is close to the C5═C6 region of a neighboring base. It is intriguing to ask if formation of the alkoxy radical may be a precursor to any of the other radicals observed in 5′dCMP (perhaps by protonation of a base anion to yield an H-addition radical). Presently, however, there are no results that link the decay of the alkoxy radical with any of the other radicals.

Finally there is the 3αH radical, best observed in 5′dCMP by irradiation at room temperature. A paper by Herak et al.[49] claims that the 3αH radical forms upon decay of radical **R6**. In the present study there is no new information to prove or disprove this claim. The warming experiments did not produce sufficient yields of the 3αH radical for study.

Acknowledgment. We thank William Bernhard, University of Rochester, for help with the first phase of this work and for helpful discussions along the way. We also thank Paul Cullis, Leicester University, for suggesting that a 5-methyl deoxycytidine impurity may be present in stock samples of nucleic acids, and Steve Swarts, Bowman Gray School of Medicine, for analyzing our stock samples and crystals for this impurity. This work is supported by PHS Grant R01 CA36810-12 awarded by the National Cancer Institute, DHHS. Partial support came from NATO Travel Grant 0426/88.

References and Notes

(1) Hüttermann, J.; Voit, K.; Oloff, H.; Kohnlein, W.; Gräslund, A.; Rupprecht, A. *Discuss. Faraday Soc.* **1984**, *78*, 135.

(2) Zell, I.; Hüttermann, J.; Gräslund, A.; Rupprecht, A.; Köhnlein, W. *Free Rad. Res. Commun.* **1989**, *6*, 2.

(3) Bernhard, W. A. *J. Phys. Chem.* **1989**, *93*, 2187.

(4) Sevilla, M. D.; Becker, D.; Yan, M.; Summerfield, S. R. *J. Phys. Chem.* **1991**, *95*, 3409.

(5) Barnes, J. P.; Bernhard, W. A. *J. Phys. Chem.* **1994**, *98*, 887.

(6) Close, D. M. *Radiat. Res.* **1993**, *135*, 1.

(7) Bernhard, W. A. *Adv. Radiat. Biol.* **1981**, *9*, 199.

(8) Becker, D.; Sevilla, M. D. *The Chemical Consequences of Radiation Damage to DNA*; Academic Press: New York, 1993; Vol. 17.

(9) Steenken, S. *Free Rad. Res. Commun.* **1992**, *16*, 349.

(10) Sagstuen, E.; Hole, E. O.; Nelson, W. H.; Close, D. M. *J. Phys. Chem.* **1992**, *96*, 8269.

(11) Close, D. M.; Bernhard, W. A. *J. Chem. Phys.* **1979**, *70*, 210.

(12) Weiland, B.; Hüttermann, J.; Malone, M. E.; Cullis, P. M. *Int. J. Radiat. Biol.* **1996**, *70*, 327.

(13) Malone, M. E.; Cullis, P. M.; Symons, M. C. R.; Parker, A. W. *J. Phys. Chem.* **1995**, *99*, 9299.

(14) Viswamitra, M. A.; Reddy, B. S.; Lin, G. H. Y.; Sundaralingam, M. *J. Am. Chem. Soc.* **1971**, *93*, 4565.

(15) Schonland, D. S. *Proc. Phys. Soc., London, Sect. A* **1959**, *73*, 788.

(16) Weil, J. A.; Schindler, P.; Wright, P. M. *Rev. Sci. Instrum.* **1967**, *38*, 659.

(17) Close, D. M.; Fouse, G. W.; Bernhard, W. A. *J. Chem. Phys.* **1977**, *66*, 1534.

(18) Nelson, W. H.; Hole, E. O.; Sagstuen, E.; Close, D. M. *Int. J. Radiat. Biol.* **1988**, *54*, 963.

(19) Lefebvre, R.; Maruani, J. *J. Chem. Phys.* **1965**, *42*, 1480.

(20) McConnell, H. M.; Chesnut, D. B. *J. Chem. Phys.* **1958**, *28*, 107.

(21) Bernhard, W. A. *J. Chem. Phys.* **1984**, *81*, 5928.

(22) Nelson, W. H.; Gill, C. *Mol. Phys.* **1978**, *36*, 1779.

(23) Lessard, J.; Griller, D.; Ingold, K. U. *J. Am. Chem. Soc.* **1980**, *102*, 326.

(24) Box, H. C.; Budzinski, E. E.; Potienko, G. *J. Chem. Phys.* **1980**, *73*, 2052.

(25) Rustgi, S. N.; Box, H. C. *J. Chem. Phys.* **1974**, *60*, 3343.

(26) Huuse, N. I.; Sagstuen, E. Unpublished results.

(27) Close, D. M. *Radiat. Res.* **1997**, *147*, 663.

(28) Krilov, D.; Herak, J. N. *Biochim. Biophys. Acta* **1974**, *366*, 396.

(29) McConnell, H. M.; Heller, C.; Cole, T.; Fessenden, R. W. *J. Am. Chem. Soc.* **1960**, *82*, 766.

(30) Herak, J. N.; Lenard, D. R.; McDowell, C. A. *J. Magn. Reson.* **1977**, *26*, 189.

(31) Box, H. C.; Potter, W. R.; Budzinski, E. E. *J. Chem. Phys.* **1975**, *62*, 3476.

(32) Box, H. C. *Faraday Discuss.* **1977**, *63*, 264.

(33) Hole, E. O.; Nelson, W. H.; Sagstuen, E.; Close, D. M. *Radiat. Res.* **1997**, *149*, 109.

(34) Close, D. M.; Nelson, W. H.; Sagstuen, E. *Radiat. Res.* **1987**, *112*, 283.

(35) McCalley, R. C.; Kwiram, A. L. *J. Phys. Chem.* **1993**, *97*, 2888.

(36) Bernhard, W. A.; Barnes, J.; Mercer, K. R.; Mroczka, N. *Radiat. Res.* **1994**, *140*, 199.

(37) Krilov, D.; Velenik, A.; Herak, J. N. *J. Chem. Phys.* **1978**, *69*, 2420.

(38) Hüttermann, J. *Ultramicroscopy* **1982**, *10*, 25.

(39) Bernhard, W. A.; Close, D. M.; Hüttermann, J.; Zehner, H. *J. Chem. Phys.* **1977**, *67*, 1211.

(40) Hole, E. O.; Nelson, W. H.; Sagstuen, E.; Close, D. M. *Radiat. Res.* **1992**, *129*, 119.

(41) Kerr, C. M. L.; Webster, K.; Williams, F. *J. Phys. Chem.* **1972**, *76*, 2848.

(42) Hampton, D. A.; Alexander, C., Jr. *J. Chem. Phys.* **1973**, *58*, 4891.

(43) Bernhard, W. A.; Hüttermann, J. A.; Müller, A.; Close, D., M.; Fouse, G. W. *Radiat. Res.* **1976**, *68*, 390.

(44) Close, D. M.; Fouse, G. W.; Bernhard, W. A. *J. Chem. Phys.* **1977**, *66*, 4689.

(45) Sevilla, M. D. *J. Phys. Chem.* **1971**, *75*, 626.

(46) Hüttermann, J. *Int. J. Radiat. Biol.* **1970**, *17*, 249.

(47) Cullis, P. M. Personal communication.

(48) Swarts, S. Personal communication.

(49) Herak, J. N.; Krilov, D.; McDowell, C. A. *J. Magn. Reson.* **1976**, *23*, 1.

(50) Hole, E. O.; Sagstuen, E.; Nelson, W. H.; Close, D. M. *J. Phys. Chem.* **1991**, *95*, 1494.

(51) Close, D. M.: Bernhard, W. A. Unpublished results.